IEEE Access
Multidisciplinary ⋮ Rapid Review ⋮ Open Access Journal

Received July 22, 2020, accepted August 8, 2020, date of publication August 11, 2020, date of current version August 21, 2020.

Digital Object Identifier 10.1109/ACCESS.2020.3015773

A New Matrix Projective Synchronization of Fractional-Order Discrete-Time Systems and Its Application in Secure Communication

WENHAO YAN AND QUN DING
Electronic Engineering College, Heilongjiang University, Harbin 150080, China
Corresponding author: Qun Ding (qunding@aliyun.com)

This work was supported by the National Natural Science Foundation of China under Grant 61471158.

ABSTRACT In this study, it is proposed that a new matrix projective synchronization of fractional-order (FO) chaotic maps in discrete-time. A new synchronization error is introduced and a control law is constructed, which makes the synchronization error converge towards zero in sufficient time under the stability theory of linearization method of FO systems. Numerical simulation results are presented to illustrate the feasibility of the scheme. Finally, a secure communication scheme based on FO discrete-time (FODT) systems was proposed.

INDEX TERMS Control law, FO calculus, FODT system, matrix projective synchronization.

I. INTRODUCTION

Chaos theory, in nonlinear dynamical systems, is a very attractive phenomenon, which has been extensively investigated and studied in the last decades. Due to its initial value sensitivity, non-periodic, continuous bandwidth spectrum, trajectory unpredictability and pseudo-random, chaos has wide application in secure communication, cryptography, image encryption, signal processing and other fields [1]–[8].

In the past three centuries, the study of fractional calculus theory has been carried out mainly in the purely theoretical field of mathematics, but in recent decades, fractional differential equations and fractional difference equations have been used more and more to describe optical and thermal systems, mechanics systems, signal processing, system identification, robotics and other applications [9]–[15]. A great number of FO chaotic maps in continuous-time and discrete-time were investigated in recent years, including FO Chen map [16], FO Rossler map [17], FO Lorenz map [18], FO Lu map [19], FO Ikeda map [20], FO Sine map [21], FO cubic Logistic map [22]. In recent years, many scholars have also studied the sliding mode control and circuit implementation of FO chaotic systems [37]–[42].

Chaos synchronization, in nonlinear science, is one of the hot topics. Since Pecora and Carroll proposed the complete synchronization method of chaotic system in 1990s, great strides have been made in chaotic synchronization [23], [24], [24]–[28], [30]. However, there are few references on the synchronization of FODT chaotic systems. In 2014, Hu [31] studied FO Henon map, which has made an unprecedented contribution to the high dimensional FODT chaotic synchronization method. In 2015, Wu and Baleanu [32] proposed synchronization of the FO Logistic map, and this synchronization method is only suitable for master-slave systems with the same dimension. In 2017, Shukla and Sharma [33] studied generalized FO Henon map and proposed active control synchronization, and this synchronization method is also only suitable for master-slave systems with the same dimension. Ouannas *et al.* [34] proposed a general synchronization of FODT chaotic systems in 2018. Though this synchronization method can be suitable for master-slave systems with different dimensions, it's hard to find the right bijection function f to meet requirement.

In order to better synchronize FODT chaotic systems with different dimensions, a new matrix projective synchronization, in this article, is proposed. This new synchronization method relies on an invertible matrix P and an arbitrary matrix M, so it is called P-M synchronization. Compared with the existing synchronization methods, P-M synchronization, constructs a controller U to make the synchronization error meet the requirements. Secondly, compared with matrix projection synchronization, P-M synchronization

The associate editor coordinating the review of this manuscript and approving it for publication was Sun Junwei.

can realize synchronization of different dimensions of the same master-slave system. Lastly, compared with one-to-one mapping f, it is easy to construct an invertible matrix P.

This article is organized as follows. In Section 2, some preliminary knowledge of discrete fractional order equations is given. In Section 3, we give the P-M synchronization criterion and the stability theory of discrete fractional order system. Section 4 present some numerical simulation results related to concrete examples to show the feasibility of this synchronization scheme. In Section 5, a secure communication scheme based on fractional-order discrete-time systems was proposed. Finally, a general summary of this article is drawn in Section 5.

II. PRELIMINARIES

The drive and response maps considered in presented article are in the following forms,

$$ {}^{C}\Delta_{a}^{\alpha}X(t) = AX(t+v-1) + \phi(X(t+v-1)), \quad \forall t \in \mathbb{N}_{a+1-\alpha} \tag{1} $$

$$ {}^{C}\Delta_{a}^{\beta}Y(t) = BY(t+v-1) + \varphi(Y(t+v-1)) + U, \quad \forall t \in \mathbb{N}_{a+1-\beta} \tag{2} $$

where the n-tuple vectors $X(t) = (x_1(t), x_2(t), \ldots, x_n(t))^T$ and the m-tuple vectors $Y(t) = (y_1(t), y_2(t), \ldots, y_m(t))^T$ are state vectors of the drive and response maps, respectively, $A \in \mathbb{R}^{n\times n}$, and $B \in \mathbb{R}^{m\times m}$ are the linear parts of the drive and response maps, respectively, and the map $\phi : \mathbb{R}^n \to \mathbb{R}^n$, $\varphi : \mathbb{R}^m \to \mathbb{R}^m$ are the nonlinear functions of the above maps and $U = (u_1, u_2, \ldots, u_m)^T$ is a vector controller, which is to be determined by the control law of the synchronization scheme.

Remark 1: v denotes the order of fractional difference equation, and $0 < v \leq 1$.

Remark 2: $\mathbb{N}_a$ denotes the set of natural numbers beginning from a. The notation ${}^{C}\Delta_{a}^{\alpha}X(t)$ denotes the Caputo type delta difference of $X(t)$ defined over $\mathbb{N}_a$.

Definition 1 [36]: Caputo type delta difference of $X(t)$ on $\mathbb{N}_a$ is defined as,

$$ {}^{C}\Delta_{a}^{v}X(t) = \frac{1}{\Gamma(n-v)} \sum_{s=a}^{t-(n-v)} (t-\sigma(s))^{(n-v-1)} \Delta_{s}^{n}X(s) \tag{3} $$

where $n = [a] + 1$, $\sigma(s) = s + 1$, and the notation $\Delta_{s}^{n}X(s)$ denotes the v-th fractional sum of x_i.

Lemma 1 [37]: The Caputo type delta difference in the form of equation (4) below is equivalent to the discrete integral equation in the form of equation (5) below.

$$ \begin{cases} {}^{C}\Delta_{a}^{v}u(t) = f(t+v-1, u(t+v-1)) \\ \Delta^{k}u(a) = u_k, n = [v]+1, k = 0, 1, \ldots .n-1 \end{cases} \tag{4} $$

$$ u(t) = u_0(t) + \frac{1}{\Gamma(v)} \sum_{s=a+n-v}^{t-v} (t-\sigma(s))^{(v-1)} \times f(s+v-1, u(s+v-1)), \tag{5} $$

where $\sigma(s) = s+1$, $t \in \mathbb{N}_{a+n}$, and $u_0(t) = \sum_{k=0}^{n-1} \frac{(t-a)^{(k)}}{k!} u_k$.

III. STABILITY CRITERIA FOR DISCRETE FRACTIONAL ORDER LINEAR SYSTEMS

In this section, we will introduce a new matrix projective synchronization based on FODT chaotic system.

Definition 1: Matrix projective synchronization is said to be achieved between drive system (1) and response system (2) if there exists a matrix $M \in \mathbb{R}^{m\times n}$ such that the dynamic synchronization error

$$ \lim_{t\to\infty} \|e(t) := Y(t) - MX(t)\| = 0. \tag{6} $$

Based on matrix projection synchronization, we propose a new synchronization scheme, namely, *P-M* synchronization.

Definition 2: P-M synchronization is said to be achieved between drive system (1) and response system (2) if there exists an invertible matrix $P \in \mathbb{R}^{n\times n}$ and a matrix $M \in \mathbb{R}^{m\times n}$ such that the dynamic synchronization error

$$ e(t) := PY(t) - MX(t) \tag{7} $$

satisfies the condition $\lim_{t\to\infty} \|e(t) = 0\|$.

The v order Caputo fractional difference of equation (7) is as the following form.

$$ \begin{aligned} {}^{C}\Delta^{v}e(t) &= {}^{C}\Delta^{v}(PY(t) - MX(t)) \\ &= PBY(t+v-1) + P\phi(t+v-1) + PU \\ &\quad -MAX(t+v-1) + M\varphi(t+v-1) \end{aligned} \tag{8} $$

Equation (8) can be further derived as follows:

$$ {}^{C}\Delta^{v}e(t) = (B-C)e(t+v-1) + P \times U + R, \tag{9} $$

where $C \in \mathbb{R}^{m\times m}$ is a control matrix and

$$ R = (C-B)e(t) + PBY(t) + P\varphi(t) - MAX(t) - M\phi(t). \tag{10} $$

Lemma 1 [38]: The zero equilibrium of the linear fractional order discrete system:

$$ {}^{C}\Delta^{v}e(t) = Me(t+v-1), \tag{11} $$

is asymptotically stable, if

$$ \lambda \in \left\{ z \in \mathbb{C} : |z| < \left(2\cos\frac{|\arg z| - \pi}{2-v}\right)^{v} \textit{ and } \ |\arg z| > \frac{v\pi}{2} \right\}, \tag{12} $$

where $e(t) \in \mathbb{R}^n$, $0 < v \leq 1$, $M \in \mathbb{R}^{n\times n}$, $\forall t \in \mathbb{N}_{a+1-v}$ and λ is the eigenvalues of the matrix M. Based on Lemma 3.1, *P-M* synchronization can be achieved if there exists a controller U such that the eigenvalues of the coefficient matrix of the error function $e(t)$ meet the requirements of equation (12). Next, we are now ready to present the *P-M* synchronization.

Theorem 1: system (1) and (2) can be achieved *P-M* synchronization if

$$ U = -QR \tag{13} $$

where matrix Q is the inverse of matrix P and the control matrix C is chosen such that all the eigenvalues λ of the matrix $(B-C)$ is satisfy

$$ -2^{v} < \lambda < 0. \tag{14} $$

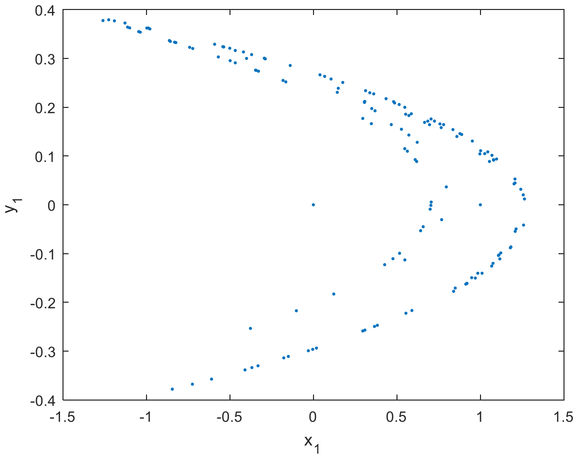

FIGURE 1. x-y phase space of the 2D FO generalized Henon map.

Proof. By substituting equation (10) into equation (9), the synchronization error system (8) reduces to

$$^{C}\Delta^{v}e(t) = (B - C)\, e(t + v - 1). \tag{15}$$

Furthermore, according to the equation (14), it is easy to see that all eigenvalues of the matrix $(B - C)$ satisfy

$$|\arg\lambda| = \pi > \frac{v\pi}{2}, \quad \text{and } |\lambda| < \left(2\cos\frac{|\arg\lambda| - \pi}{2 - v}\right)^{v}. \tag{16}$$

IV. NUMERICAL EXAMPLES

In this section, we consider some numerical examples to show the validity of synchronization scheme illustrated above. The 2D FO Henon map as expressed in [32] is given by:

$$\begin{cases} ^{C}\Delta_{a}^{v}x_1(t) = x_2(t + v - 1) + 1 - a_1x_1^2(t + v - 1) \\ \qquad -x_1(t + v - 1) \\ ^{C}\Delta_{a}^{v}x_2(t) = b_1x_1(t + v - 1) - x_2(t + v - 1), \end{cases} \tag{17}$$

when parameter $v = 0.984$ and $(a_1, b_1) = (1.4, 0.3)$, The FO Henon map exhibits chaotic behavior. The phase portrait with the initial values $(x_1(0), x_2(0)) = (0, 0)$ is depicted in Fig.1. It can be seen from Fig. 1 that the 2D FO Henon map become chaotic under certain parameters. The 3D FO generalized Henon map as expressed in [34] is given as

$$\begin{cases} ^{C}\Delta_{a}^{v}x_1(t) = -b_2x_3(t + v - 1) - x_1(t + v - 1) \\ ^{C}\Delta_{a}^{v}x_2(t) = b_2x_3(t + v - 1) + x_1(t + v - 1) \\ \qquad -x_2(t + v - 1) \\ ^{C}\Delta_{a}^{v}x_3(t) = 1 + x_2(t + v - 1) + a_2(x_3(t + v - 1))^2 \\ \qquad -x_3(t + v - 1), \end{cases} \tag{18}$$

when the parameters $(a_2, b_2) = (0.99, 0.2)$ and the order $v = 0.984$, system (18) is chaotic system. The chaotic trajectories is shown in Fig.2 with the initial values $(x_1(0), x_2(0), x_3(0)) = (0.1, 0.2, 0.5)$. It can be seen from Fig. 2 that the 3D FO Henon map become chaotic under certain parameters.

A. P-M SYNCHRONIZATION IN 3D

In order to unify the notation, equation (17) can be rewritten as the following expression:

$$^{C}\Delta_{a}^{v}X(t) = AX(t) + \phi(X(t)), \tag{19}$$

where

$$A = \begin{pmatrix} -1 & 1 \\ -b_1 & -1 \end{pmatrix} \quad \text{and } \phi = \begin{pmatrix} 1 - a_1x_1^2(t) \\ 0 \end{pmatrix}. \tag{20}$$

The 3D FO Henon map is selected as response system. Map (18) can be written as

$$^{C}\Delta_{a}^{v}Y(t) = By(t) + \varphi(Y(t)) + U, \tag{21}$$

where

$$B = \begin{pmatrix} -1 & 0 & -b_2 \\ 1 & -1 & b_2 \\ 0 & 1 & -1 \end{pmatrix} \text{and} \varphi = \begin{pmatrix} 0 \\ 0 \\ 1 - a_2x_3^2(t) \end{pmatrix}. \tag{22}$$

Given the approach presented in last section, the error system is given by

$$(e_1(t), e_2(t), e_3(t))^T = P_1(y_1(t), y_2(t), y_3(t))^T \\ -M_1(x_1(t), x_2(t))^T, \tag{23}$$

where matrix P_1 and M_1 are selected as followings:

$$P_1 = \begin{pmatrix} 1 & 0 & 0 \\ 0 & 1 & 0 \\ 0 & 0 & 1 \end{pmatrix}, \quad M_1 = \begin{pmatrix} 1 & 2 \\ 3 & 4 \\ 5 & 6 \end{pmatrix}. \tag{24}$$

Based on our approach proposed in Section 3, a control matrix C_1 is selected such that the whole eigenvalues of matrix $(B - C_1)$ satisfy the condition of Theorem 3.1. Matrix C_1 is selected as following:

$$C_1 = \begin{pmatrix} 0 & 0 & 0 \\ 1 & 0 & 0 \\ 0 & 1 & 0 \end{pmatrix}, \tag{25}$$

then, the error system is given by

$$\begin{pmatrix} ^{C}\Delta^{v}e_1(t) \\ ^{C}\Delta^{v}e_2(t) \\ ^{C}\Delta^{v}e_3(t) \end{pmatrix} = \begin{pmatrix} -1 & 0 & -b_2 \\ 0 & -1 & b_2 \\ 0 & 0 & -1 \end{pmatrix} \begin{pmatrix} e_1(t + v - 1) \\ e_2(t + v - 1) \\ e_3(t + v - 1) \end{pmatrix}. \tag{26}$$

It easy to say that the whole eigenvalues of matrix $(B - C_1)$ satisfy the condition of Theorem 3.1. The initial value of the error iteration is given

$$\begin{pmatrix} e_1(0) \\ e_2(0) \\ e_3(0) \end{pmatrix} = \begin{pmatrix} 0.1 \\ 0.2 \\ 0.5 \end{pmatrix}. \tag{27}$$

The synchronization error of system (17) and (18) is depicted in Fig.3. It is clear to see that the synchronization error quickly converges to a very small value that satisfies the requirement, which indicate that drive system (17) and response system (18) can achieve *P-M* synchronization in 3 dimensions.

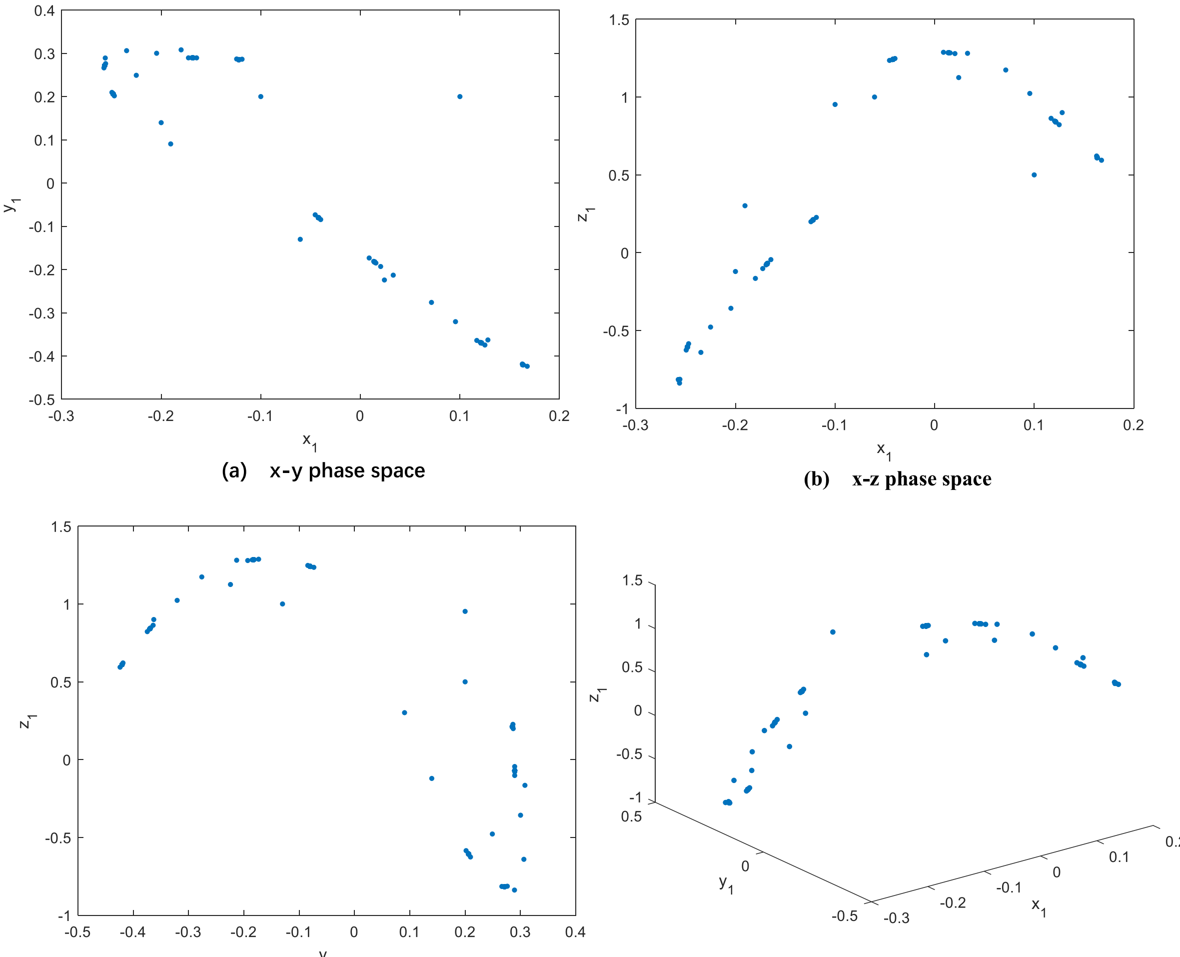

(a) x-y phase space (b) x-z phase space (c) y-z phase space (d) x-y-z phase space

FIGURE 2. Phase space of the 3D FO generalized Henon map.

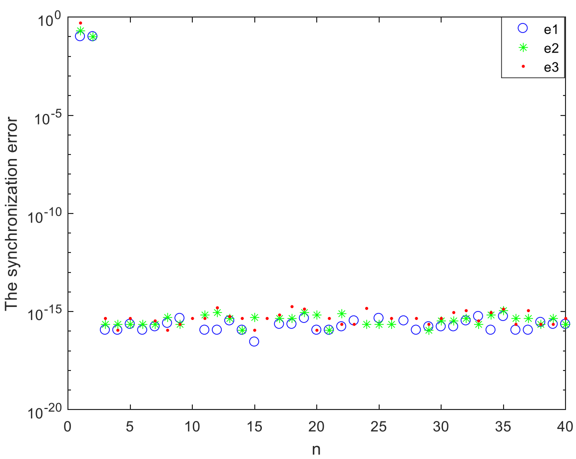

FIGURE 3. The synchronization error of the discrete-time system.

B. P-M SYNCHRONIZATION IN 2D

The 3D FO Henon map is selected as drive system, and the 2D FO Henon map is selected as response system. We are just interchanging the matrix A and B, and the mapping ϕ and φ, so we are not dividing the linear part from the nonlinear part.

Given the approach presented in last section, the error system is given by

$$(e_1(t),\ e_2(t))^T = P_2(y_1(t),\ y_2(t))^T - M_2(x_1(t),\ x_2(t),\ x_3(t))^T, \tag{28}$$

where matrix P_2 and M_2 are selected as followings:

$$P_2 = \begin{pmatrix} 1 & 0 \\ 0 & 1 \end{pmatrix}, \quad M_2 = \begin{pmatrix} 1 & 2 & 3 \\ 4 & 5 & 6 \end{pmatrix}. \tag{29}$$

Matrix C_2 is selected as following:

$$C_2 = \begin{pmatrix} 0 & 1 \\ 0.3 & -0.5 \end{pmatrix}, \tag{30}$$

then, the error system is given by

$$\begin{pmatrix} {}^C\Delta^v e_1(t) \\ {}^C\Delta^v e_2(t) \end{pmatrix} = \begin{pmatrix} -1 & 0 \\ 0 & -\frac{1}{2} \end{pmatrix} \begin{pmatrix} e_1(t+v-1) \\ e_2(t+v-1) \end{pmatrix}. \tag{31}$$

The initial value of the error iteration is given as follows:

$$\begin{pmatrix} e_1(0) \\ e_2(0) \end{pmatrix} = \begin{pmatrix} -2 \\ -4.4 \end{pmatrix}. \tag{32}$$

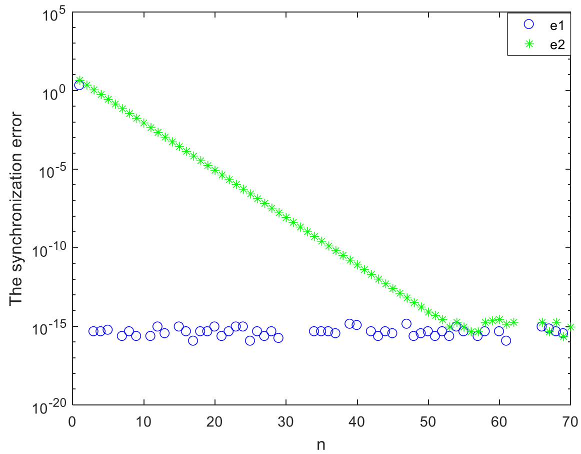

FIGURE 4. The synchronization error of the discrete-time system.

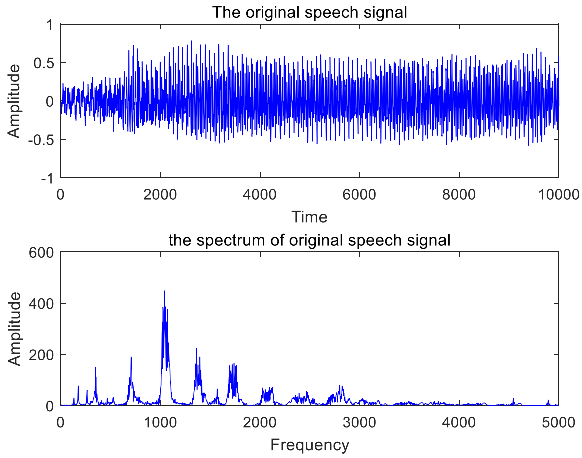

FIGURE 5. The original speech signal.

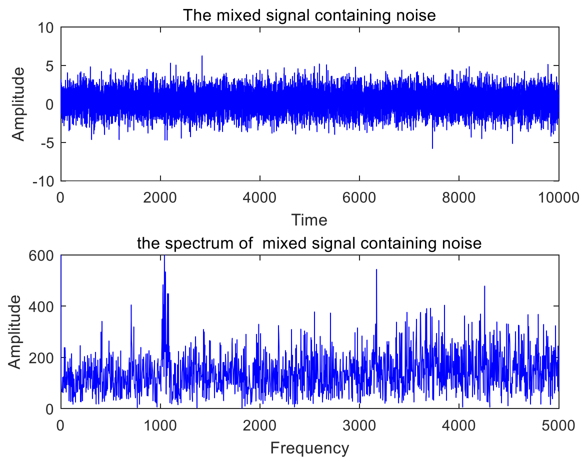

FIGURE 6. The mixed signal containing noise.

The synchronization error of system (18) and (17) is depicted in Fig.4. It is clear to see that the synchronization error quickly converges to a very small value that satisfies the requirement, which indicate that drive system (18) and response system (17) can achieve *P-M* synchronization in 2 dimensions.

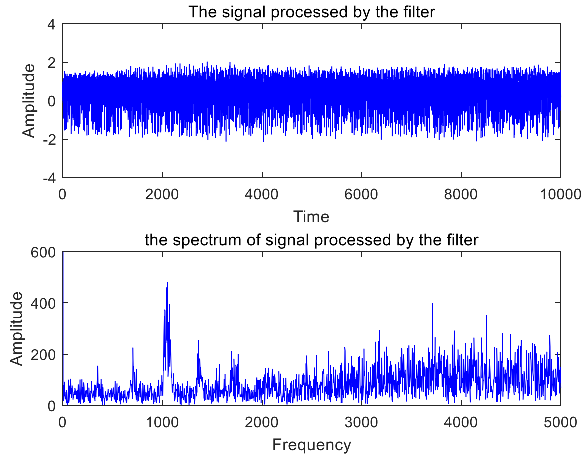

FIGURE 7. The signal processed by the filter.

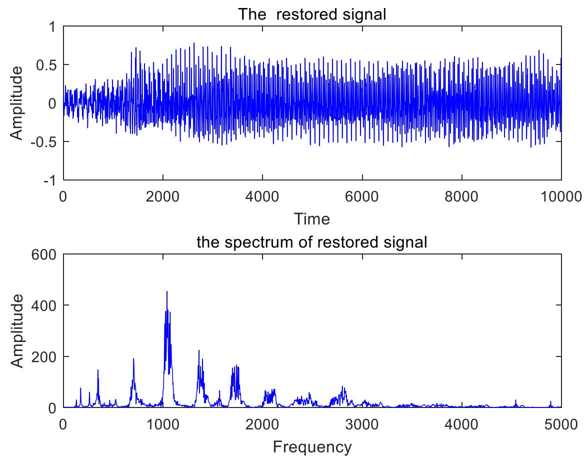

FIGURE 8. The restored signal.

V. A SECURE COMMUNICATION SCHEME BASED ON FODT SYSTEMS

A. THE SPEECH ENCRYPTION SCHEME

Secure communications can be classified into three major security technologies: chaotic masking technology, chaotic parameter modulation technology and chaotic keying technology. Chaos masking technology belongs to chaos analog communication, chaos parameter modulation and chaos keying technology belongs to chaos digital communication technology. Compared with chaotic parameter modulation technology and chaotic keying technology, chaos masking is easy to implement, short encryption time and low complexity because it is simple addition and subtraction. The speech encryption scheme is mainly based on chaos masking, and the block diagram of communication is shown in Fig.9.

The FO discrete-time chaotic map (19) is used as master system, and map (21) is used as slave system. Speech signal $s(t)$ and state variable ${}^{C}\Delta_a^{v}X(t)$ are masked into the signal $E(t)$, then, the signal $E(t)$ is sent to the receiver end via the public channel. However, the transmission channel will be contaminated by chaotic noise. Suppose the noise is White Gaussian Noise $w(t)$.At receiver end, the recovered signal

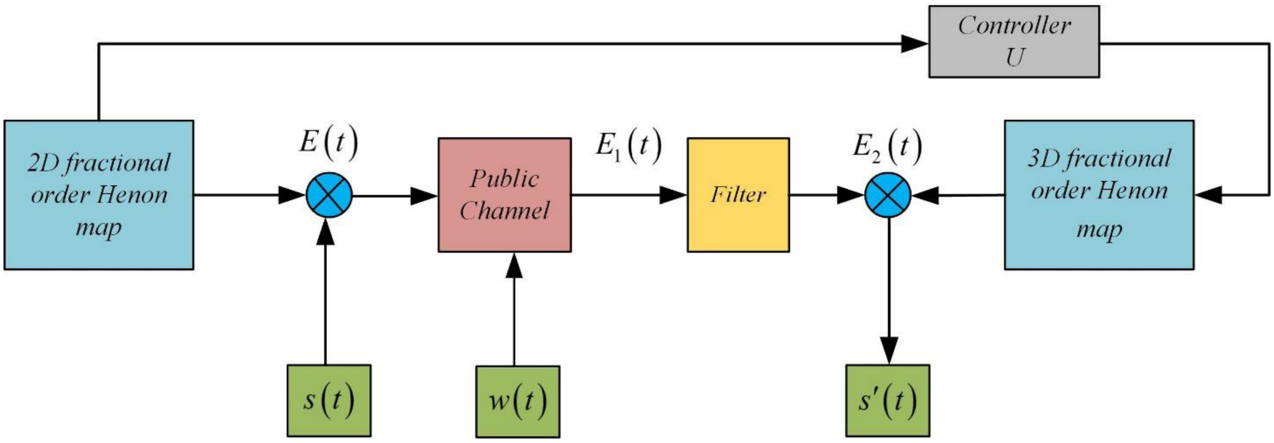

FIGURE 9. Discrete chaotic secure communication scheme.

$s'(t)$ can be obtained through the signal $E_2(t)$ and state variable ${}^{C}\Delta_a^v Y(t)$, where $E_2(t)$ is the signal processed by a filter.

$$E(t) = s(t) + {}^{C}\Delta_a^v x_1(t) + 2\,{}^{C}\Delta_a^v x_2(t) \quad (33)$$

$$E_1(t) = E(t) + w(t) \quad (34)$$

$$s'(t) = E_2(t) - {}^{C}\Delta_a^v y_1(t) \quad (35)$$

Let the initial values of the systems (19) and (21) be: $(e_1(0), e_2(0), e_3(0))^T = (0.1, 0.2, 0.5)^T$. The time-domain and frequency-domain values of the speech signals at each stage were simulated, and the simulation results were shown in Fig.5, Fig.6, Fig.7, Fig.8, respectively.

Fig.5 and Fig.8 proved that *P-M* synchronization in 3D proposed in this article can be applied into secure communication field from time domain and frequency domain.

B. SECURITY ANALYSIS

1) KEY SPACE ANALYSIS

The initial keys of this encryption scheme are the initial values of master system x_0, y_0 and the order of master system v, respectively Floating point accuracy is 10^{-15}, then the key space is 10^{45}, which is much larger than 100 2 Therefore, this scheme can provide security in terms of key space.

2) SENSITIVITY ANALYSIS OF KEYS

According to the principle of cryptography, the stronger the sensitivity of the key, the stronger the ability to resist differential attacks Generally speaking, the small difference of the same plaintext encryption key can cause a huge change of the ciphertext sequence; the slight difference of the same ciphertext decryption key can cause the decryption results are quite different First, the encryption key $r = (x_1(0), x_2(0)) = (0, 0)$ is used to complete the encryption operation of the encryption scheme, and then the error decryption key $r' = (r_1, r_2, r_3)$ of the small difference is selected, where $r_1 = \left(0 + 10^{-15}, 0\right)$, $r_2 = \left(0,\ 0 + 10^{-15}\right)$ and $r_3 = \left(0 + 10^{-15},\ 0 + 10^{-15}\right)$.

TABLE 1. The mean square error of error decryption signal relative to original voice signal.

r	r_1	r_2	r_3
2.3×10^{-4}	3.2×10^{3}	4.7×10^{3}	3.6×10^{5}

Let the original speech signal be $p_{(i)}$ and the decrypted speech signal be $p'_{(i)}$, then their mean square error is as

$$E_{MS} = \frac{1}{N}\sum_{i=0}^{N-1}\left[p'(i) - p(i)\right]^2. \quad (36)$$

The mean square error of the r' decrypted signal and the original speech signal calculated by "(36)" is shown in Table 1 It can be seen that the decryption key has a slight error, and the decryption result will be completely different, that is, the key sensitivity of the algorithm is numerically proved.

3) PHASE SPACE RECONSTRUCTION ATTACK

This scheme can resist the phase space reconstruction attack Because the mixed signal that the original speech signal after chaos masking $E(t)$ is transmitted in the common channel, the phase space reconstructed from a series of values of $E(t)$ is not completely topologically equivalent to the real chaotic system.

4) ROBUSTNESS

The robustness of this scheme is poor, since the chaotic system is sensitive to the initial value and system parameters If the system parameters are changed, the output of the chaotic system will change Furthermore, from the perspective of secure communication, if the system has better robustness, it will lose confidentiality.

VI. CONCLUSION

In this article, we proposed a new matrix projective of fractional-order discrete-time chaotic maps of different dimensions. Compared with matrix projection synchron-ization, this synchronization can synchronize any n-dimensional chaotic map (drive system) with m-dimensional chaotic system (response system) by selecting an invertible matrix $P \in \mathbb{R}^{n\times n}$ and an arbitrary matrix $M \in \mathbb{R}^{m\times n}$. Numerical simulation results in Section 4 have shown the validity of this synchronization scheme. In Section 5, a secure communication scheme based on fractional-order discrete-time systems was proposed, and through numerical simulation results confirmed the feasibility of the scheme. In the future work, we intend to implement the secure communication scheme mentioned in this article on the hardware circuit.

REFERENCES

[1] X. Wu, Y. Li, and J. Kurths, "A new color image encryption scheme using CML and a fractional-order chaotic system," *PLoS ONE*, vol. 10, no. 3, pp. 119660–119687, 2015.

[2] X. Wang, C. Liu, and D. Xu, "Image encryption scheme using chaos and simulated annealing algorithm," *Nonlinear Dyn.*, vol. 84, no. 3, pp. 1–13, 2016.

[3] A. Kiani-B, K. Fallahi, N. Pariz, and H. Leung, "A chaotic secure communication scheme using fractional chaotic systems based on an extended fractional Kalman filter," *Commun. Nonlinear Sci. Numer. Simul.*, vol. 14, no. 3, pp. 863–879, Mar. 2009.

[4] H. Liu, S. Li, H. Wang, Y. Huo, and J. Luo, "Adaptive synchronization for a class of uncertain fractional-order neural networks," *Entropy*, vol. 17, no. 12, pp. 7185–7200, Oct. 2015.

[5] C. Liu, L. Ding, and Q. Ding, "Research about the characteristics of chaotic systems based on multi-scale entropy," *Entropy*, vol. 21, p. 663, Jul. 2019.

[6] G. Wen, G. Grassi, Z. Feng, and X. Liu, "Special issue on advances in nonlinear dynamics and control," *J. Franklin Inst.*, vol. 352, no. 8, pp. 1985–2986, 2015.

[7] R. Martínez-Guerra, J. J. M. García, and S. M. D. Prieto, "Secure communications via synchronization of Liouvillian chaotic systems," *J. Franklin Inst.*, vol. 353, no. 17, pp. 4384–4399, Nov. 2016.

[8] L. Ding, C. Liu, Y. Zhang, and Q. Ding, "A new lightweight stream cipher based on chaos," *Symmetry*, vol. 11, no. 7, p. 853, Jul. 2019.

[9] R. Gorenlo and F. Mainardi, *Fractional Calculus*. Berlin, Germany: Springer, 1997, pp. 123–157.

[10] R. Magin, *Fractional Calculus in Bioengineering*. New York, NY, USA: Begell House Redding, 2006, pp. 75–127.

[11] A. G. Radwan, A. Shamim, and K. N. Salama, "Theory of fractional order elements based impedance matching networks," *IEEE Microw. Wireless Compon. Lett.*, vol. 21, no. 3, pp. 120–122, Mar. 2011.

[12] T. Abdeljaward, "On Riemann and Caputo fractional differences," *Comput. Math. Appl.*, vol. 62, no. 3, pp. 1602–1622, 2011.

[13] G.-C. Wu, D. Baleanu, H.-P. Xie, and F.-L. Chen, "Chaos synchronization of fractional chaotic maps based on the stability condition," *Phys. A, Stat. Mech. Appl.*, vol. 460, pp. 374–383, Oct. 2016.

[14] A. Azarang, S. Kamaei, M. Miri, and M. H. Asemani, "A new fractional-order chaotic system and its synchronization via Lyapunov and improved Laplacian-based method," *Optik*, vol. 127, no. 24, pp. 11717–11731, Dec. 2016.

[15] O. Megherbi, H. Hamiche, S. Djennoune, and M. Bettayeb, "A new contribution for the impulsive synchronization of fractional-order discrete-time chaotic systems," *Nonlinear Dyn.*, vol. 90, no. 3, pp. 1519–1533, Nov. 2017.

[16] C. Li and G. Peng, "Chaos in Chen's system with a fractional order," *Chaos, Solitons Fractals*, vol. 22, no. 2, pp. 443–450, Oct. 2004.

[17] C. Li and G. Chen, "Chaos and hyperchaos in the fractional-order Rössler equations," *Phys. A, Stat. Mech. Appl.*, vol. 341, pp. 55–61, Oct. 2004.

[18] I. Grigorenko and E. Grigorenko, "Chaotic dynamics of the fractional Lorenz system," *Phys. Rev. A, Gen. Phys.*, vol. 91, no. 3, Jul. 2003, Art. no. 034101.

[19] J. Wang and Y. Zhang, "Designing synchronization schemes for chaotic fractional-order unified systems," *Chaos, Solitons Fractals*, vol. 30, no. 5, pp. 1265–1272, Dec. 2006.

[20] A. Ouannas, A.-A. Khennaoui, Z. Odibat, V.-T. Pham, and G. Grassi, "On the dynamics, control and synchronization of fractional-order Ikeda map," *Chaos, Solitons Fractals*, vol. 123, pp. 108–115, Jun. 2019.

[21] G.-C. Wu, D. Baleanu, and S.-D. Zeng, "Discrete chaos in fractional sine and standard maps," *Phys. Lett. A*, vol. 378, nos. 5–6, pp. 484–487, Jan. 2014.

[22] C. Liu, L. Huang, and K. Wu, "Chaos in discrete cubic logistic map and bifurcation analysis," *J. Comput. Complex. Appl.*, vol. 1, no. 2, pp. 105–111, 2015.

[23] L. M. Pecora and T. L. Carroll, "Synchronization in chaotic systems," *Phys. Rev. A, Gen. Phys.*, vol. 64, no. 8, pp. 821–824, 1990.

[24] A. Ouannas, "A new generalized-type of synchronization for discrete-time chaotic dynamical systems," *J. Comput. Nonlinear Dyn.*, vol. 10, no. 6, Nov. 2015, Art. no. 061019.

[25] W. Yan and Q. Ding, "A new matrix projective synchronization and its application in secure communication," *IEEE Access*, vol. 7, pp. 112977–112984, 2019.

[26] G. Li and H. Liu, "Stability analysis and synchronization for a class of fractional-order neural networks," *Entropy*, vol. 18, no. 2, p. 55, Feb. 2016.

[27] X. He, C. Li, J. Huang, and L. Xiao, "Generalized synchronization of arbitrary-dimensional chaotic systems," *Optik-Int. J. Light Electron Opt.*, vol. 126, no. 4, pp. 454–459, Feb. 2015.

[28] S. M. Berber, "Discrete time domain analysis of chaos-based wireless communication systems with imperfect sequence synchronization," *Signal Process.*, vol. 154, pp. 198–206, Jan. 2019.

[29] M. Han, M. Zhang, and Y. Zhang, "Projective synchronization between two delayed networks of different sizes with nonidentical nodes and unknown parameters," *Neurocomputing*, vol. 171, no. 1, pp. 605–614, Jan. 2016.

[30] A. Ouannas, Z. Odibat, N. Shawagfeh, A. Alsaedi, and B. Ahmad, "Universal chaos synchronization control laws for general quadratic discrete systems," *Appl. Math. Model.*, vol. 45, pp. 636–641, May 2017.

[31] T. Hu, "Discrete chaos in fractional henon map," *Appl. Math.*, vol. 5, no. 15, pp. 2243–2248, 2014.

[32] G.-C. Wu and D. Baleanu, "Reprint of: Chaos synchronization of the discrete fractional logistic map," *Signal Process.*, vol. 107, pp. 444–447, Feb. 2015.

[33] M. Shukla and B. Sharma, "Investigation of chaos in fractional order generalized hyperchaotic Henon map," *AEU-Int. J. Electron. C*, vol. 78, pp. 256–273, Aug. 2017.

[34] A. Ouannas, A. Khennaoui, G. Grassi, and S. Bendoukha, "On the Q-S chaos synchronization of fractional-order discrete-time systems: General method and examples," *Discrete Dyn. Nat. Soc.*, vol. 2018, no. 9, 2018, Art. no. 2950357.

[35] F. M. Atici and P. Eloe, "Discrete fractional calculus with the Nabla operator," *Electron. J. Qualitative Theory Differ. Equ.*, vol. 3, pp. 1–12, 2009.

[36] J. Cermák, I. Gyori, and L. Nechvátal, "On explicit stability conditions for a linear fractional difference system," *Fractional Calculus Appl. Anal.*, vol. 18, no. 3, p. 651, Jan. 2015.

[37] S. Song, J. Park, B. Zhang, and X. Song, "Observer-based adaptive hybrid fuzzy resilient control for fractional-order nonlinear systems with time-varying delays and actuator failures," *IEEE Trans. Fuzzy Syst.*, to be published, doi: 10.1109/TFUZZ.2019.2955051.

[38] S. Song, J. H. Park, B. Zhang, X. Song, and Z. Zhang, "Adaptive command filtered neuro-fuzzy control design for fractional-order nonlinear systems with unknown control directions and input quantization," *IEEE Trans. Syst., Man, Cybern., Syst.*, early access, Feb. 4, 2020, doi: 10.1109/TSMC.2020.2967425.

[39] J. Sun, G. Han, Z. Zeng, and Y. Wang, "Memristor-based neural network circuit of full-function pavlov associative memory with time delay and variable learning rate," *IEEE Trans. Cybern.*, vol. 50, no. 7, pp. 2935–2945, Jul. 2020.

[40] J. Sun, Y. Wu, G. Cui, and Y. Wang, "Finite-time real combination synchronization of three complex-variable chaotic systems with unknown parameters via sliding mode control," *Nonlinear Dyn.*, vol. 88, no. 3, pp. 1677–1690, May 2017.

[41] J. Sun, X. Zhao, J. Fang, and Y. Wang, "Autonomous memristor chaotic systems of infinite chaotic attractors and circuitry realization," *Nonlinear Dyn.*, vol. 94, no. 4, pp. 2879–2887, Dec. 2018.

[42] N. Li, J. Sun, and Y. Wang, "A novel memcapacitor model and its application for image encryption algorithm," *J. Electr. Comput. Eng.*, vol. 2019, pp. 1–16, Apr. 2019, doi: 10.1155/2019/8146093.

WENHAO YAN received the B.S. degree in information and computing science from Northeast Petroleum University, China, in 2018. He is currently pursuing the M.S. degree in information and communication engineering from Heilongjiang University, Harbin. His research interests include nonlinear dynamics, chaos synchronization, and chaotic secure communication.

QUN DING received the Ph.D. degree in instrument science and technology from the Harbin Institute of Technology, China. She is currently a Professor with the College of Electronic Engineering, Heilongjiang University, China. She has published two books and more than 100 scientific articles in refereed journals and proceedings. Hers research interests include nonlinear dynamics and control, chaos pseudo-random sequence generator, and chaotic secure communication.